PHYSICAL REVIEW E, VOLUME 64, 045201(R)

Self-propulsion of cellular structures in chemically reacting mixtures

Tohru Okuzono and Takao Ohta
Institute for Nonlinear Sciences and Applied Mathematics, Graduate School of Science, Hiroshima University, Higashi-Hiroshima 739-8526, Japan

(Received 16 November 2000; revised manuscript received 13 June 2001; published 17 September 2001)

An alternative model of phase-separating reactive mixtures is proposed. In this model both phase separation and chemical reactions simultaneously take place and a traveling coherent structure can be formed through a Hopf bifurcation at a finite wave number. Numerical simulations show that, depending on the parameters, either lamellar or hexagonal structures travel at constant speeds in two-dimensional systems.

DOI: 10.1103/PhysRevE.64.045201 PACS number(s): 05.45.−a, 82.40.−g, 82.40.Ck

A great deal of effort has been made on the studies of pattern formation in nonlinear dissipative systems [1,2]. Reaction-diffusion systems offer some important view points in elucidating the mechanism of pattern formation, since they have simple mathematical structures and show a rich variety of patterns [3,4].

On the other hand, phase separation in condensed systems provides another mechanism of pattern formation. Domain morphology and kinetics of phase separation have been studied for many years both experimentally and theoretically [5]. In contrast to the case of reaction-diffusion systems, a pattern in a phase separation process grows indefinitely and the system approaches to the final thermal equilibrium state. However, it has been shown by theories [6–8] and experiments [9] that some chemical reactions can stabilize the steady-state morphology of phase-separating systems generating motionless periodic structures as stationary states.

Recently, Hildebrand and co-workers [10] (see also [11]) have introduced a model for the traveling nanoscale structures in surface chemical reactions. In their model, both a chemical reaction and a first-order phase transition (phase separation) simultaneously take place and the traveling stripe structure appears. They consider nonlocal attractive interactions between adsorbates. It is worth mentioning that a traveling stripe pattern has been observed experimentally in Langmuir monolayers [12], although, to our knowledge, there is no satisfactory theory to account for this phenomenon.

The aim of this paper is to propose, from a general point of view, a model system for self-propulsion of cellular structures in phase-separating reactive mixtures. In contrast to the nonlocal interaction in Ref. [10], we take the usual Cahn-Hilliard form for phase separation. Since the reaction terms are linear, our kinetic equations have a simpler structure than those in Ref. [10]. Furthermore, we will show in computer simulations that not only a lamellar structure, but also a hexagonal structure undergoes coherent self-propulsion.

A traveling hexagonal pattern has been obtained in the damped Kuramoto-Sivashinsky equation [13] and in a model equation for a neural field [14]. In these systems, the traveling structures appear as a secondary bifurcation after formation of motionless structure.

Consider a binary mixture of molecules A and B that undergoes phase separation. We assume that time evolution of the phase-separation process is well described by the Cahn-Hilliard equation for the order parameter $\psi \equiv \psi_A - \psi_B$, where ψ_A and ψ_B are the local concentration of the molecules A and B, respectively and satisfy $\psi_A + \psi_B = 1$. When the chemical reaction of the type $A \rightleftharpoons B$ takes place in the phase-separating system, the time evolution equation of the order parameter $\psi(\mathbf{r},t)$ at position $\mathbf{r}$ and time t is given by [6]

$$\frac{\partial \psi}{\partial t} = \nabla^2 \frac{\delta F}{\delta \psi} - \alpha(\psi - \psi_0), \tag{1}$$

where α and ψ_0 are constants that depend on the reaction rates and F is the free energy functional of the Ginzburg-Landau type:

$$F[\psi] = \int d\mathbf{r}\left[\frac{c}{2}(\nabla\psi)^2 + w(\psi)\right], \tag{2}$$

where c is a positive constant and $w(\psi)$ is a function of ψ with two degenerate minima. Since the growth of fluctuations with large wavelength is suppressed because of the last term in Eq. (1), the characteristic size of pattern formed can never reach a macroscopic one. In a steady state a periodic structure such as lamellar or hexagonal structures can be formed depending on the value of ψ_0 in two dimensions. It should be noted that Eq. (1) has the same form as the equation for microphase separation in block-copolymer systems [15], where periodic domain structures appear in equilibrium [16].

Now we consider a ternary system as a simple extension of the above model. The system is a mixture of A-, B-, and C-type molecules. We assume that there is a strong repulsive interaction between A and B molecules, and other interactions between molecules are quite weak compared with the A-B interaction. Let us introduce two order parameters $\psi(\mathbf{r},t) \equiv \psi_A - \psi_B$ and $\phi(\mathbf{r},t) \equiv \psi_A + \psi_B$ with the condition $\psi_A + \psi_B + \psi_C = 1$, where ψ_A, ψ_B, and ψ_C are the local concentration of A, B, and C molecules, respectively. We may write the time evolution equations for ψ and ϕ as

$$\frac{\partial \psi}{\partial t} = \nabla^2 \frac{\delta F}{\delta \psi} + f(\psi,\phi), \tag{3}$$

$$\frac{\partial \phi}{\partial t} = D_\phi \nabla^2 \phi + g(\psi,\phi), \tag{4}$$

where $f(\psi,\phi)$ and $g(\psi,\phi)$ are reaction terms (see below), and D_ϕ is the diffusion constant for ϕ. For simplicity, we assume in Eq. (3)

$$\frac{\delta F}{\delta \psi} = -D\nabla^2\psi - \tau\psi + u\psi^3, \tag{5}$$

where D, τ, and u are positive constants. Generally, τ might depend on ϕ such that phase separation is suppressed by the existence of C molecules. However, we ignore such an effect and explore nonequilibrium characters caused by the interplay between phase separation and chemical reaction.

Here we consider a hypothetical system that undergoes the following cyclic chemical reactions:

$$A \xrightarrow{\gamma_1} B \xrightarrow{\gamma_2} C \xrightarrow{\gamma_3} A, \tag{6}$$

where γ_1, γ_2, and γ_3 are the reaction rates. Each step of the above is the same type of reaction as used in Ref. [6]. Then the reaction terms in Eqs. (3) and (4) can be written as

$$f(\psi,\phi) = -\left(\gamma_1 + \frac{\gamma_2}{2}\right)\psi - \left(\gamma_1 - \frac{\gamma_2}{2} + \gamma_3\right)\phi + \gamma_3, \tag{7}$$

$$g(\psi,\phi) = \frac{\gamma_2}{2}\psi - \left(\frac{\gamma_2}{2} + \gamma_3\right)\phi + \gamma_3. \tag{8}$$

Equations (3)–(8) constitute our basic model. Hereafter, we assume, for the sake of simplicity, that the diffusion of ϕ is slow and we set $D_\phi = 0$ in Eq. (4). We also set $u = 1$ in Eq. (5). Equations (3) and (4) have an equilibrium uniform solution: $\psi = \psi_0$, $\phi = \phi_0$, where

$$\psi_0 \equiv \frac{\gamma_3(\gamma_2 - \gamma_1)}{\gamma_1\gamma_2 + \gamma_2\gamma_3 + \gamma_3\gamma_1}, \tag{9}$$

$$\phi_0 \equiv \frac{\gamma_3(\gamma_2 + \gamma_1)}{\gamma_1\gamma_2 + \gamma_2\gamma_3 + \gamma_3\gamma_1}. \tag{10}$$

It should be noted that the total amount of ψ and ϕ are conserved in time if we choose an initial condition such that $\langle\psi\rangle = \psi_0$ and $\langle\phi\rangle = \phi_0$, where $\langle\cdot\rangle$ implies the spatial average. The numerical simulations shown below will be carried out in this situation.

If one replaces ∇^2 by the minus sign in front of $\delta F/\delta\psi$ in Eq. (3), Eqs. (3) and (4) are the FitzHugh-Nagumo type equations used in the pattern dynamics far from equilibrium [1]. Thus we emphasize that the model system (3) and (4) is related, on one hand, to microphase separation in thermal equilibrium and, on the other hand, to the systems far from equilibrium.

The linear stability analysis of Eqs. (3) and (4) around the equilibrium solution gives us the coefficient matrix

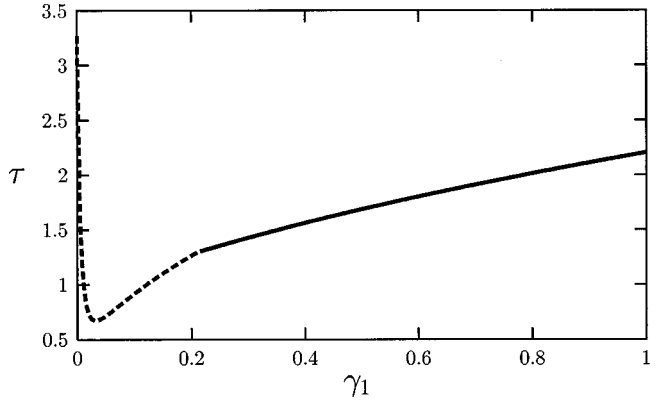

FIG. 1. Bifurcation lines in the (γ_1,τ) plane determined by $\mathrm{Re}\,\lambda(q_c) = 0$ for $D = 1.0$, $\gamma_2 = 0.2$, and $\gamma_3 = 0.01$. The solid and dashed lines show the lines at which the Hopf and Turing instabilities occur, respectively.

$$L = \begin{pmatrix} -q^2(Dq^2 - \tilde{\tau}) - \left(\gamma_1 + \frac{\gamma_2}{2}\right) & -\left(\gamma_1 - \frac{\gamma_2}{2} + \gamma_3\right) \\ \frac{\gamma_2}{2} & -\left(\frac{\gamma_2}{2} + \gamma_3\right) \end{pmatrix}, \tag{11}$$

where $\tilde{\tau} \equiv \tau - 3\psi_0^2$ and q is the magnitude of the wave vector $\mathbf{q}$ characterizing the spatial variation of ψ and ϕ.

In Fig. 1 we plot a part of bifurcation lines determined by $\mathrm{Re}\ \lambda(q_c) = 0$ in the parameter plane (γ_1,τ) for $\gamma_2 = 0.2$, $\gamma_3 = 0.01$, and $D = 1.0$, where $\lambda(q)$ is the eigenvalue of L and $q_c \equiv [\tilde{\tau}/(2D)]^{1/2}$ is the wave number that maximizes $\mathrm{Re}\,\lambda(q)$. The solid and dashed lines in this figure indicate the lines at which Hopf and Turing instability occur, respectively. For the parameters below these lines, the equilibrium solution is stable.

If an instability occurs through a Hopf bifurcation for a finite q, we can expect an oscillating periodic structure. We plot $\mathrm{Re}\,\lambda(q)$ (solid line) and $\mathrm{Im}\,\lambda(q)$ (dashed line) in Fig. 2 as functions of q^2 near the bifurcation point for $\tau = 1.7$, γ_1

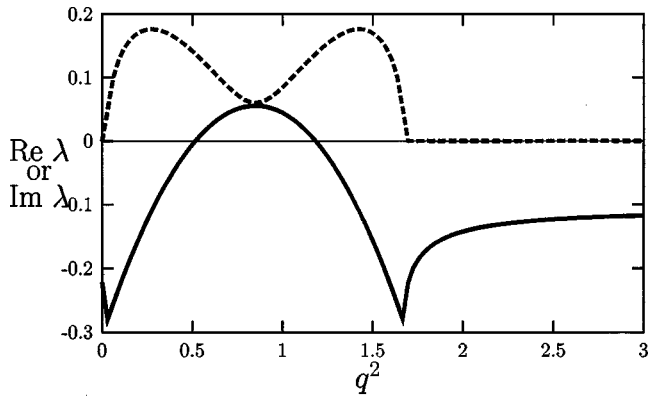

FIG. 2. The wave-number dependence of $\mathrm{Re}\,\lambda(q)$ (solid line) and $\mathrm{Im}\ \lambda(q)$ (dashed line) for $D = 1.0$, $\tau = 1.7$, $\gamma_1 = 0.4$, $\gamma_2 = 0.2$, and $\gamma_3 = 0.01$.

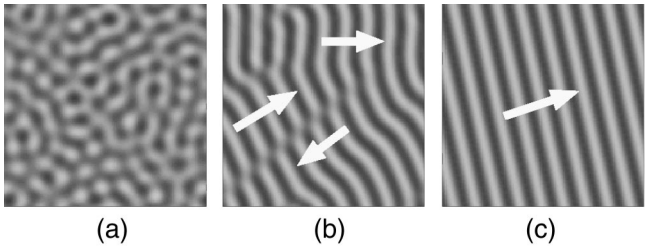

FIG. 3. Snapshots of the moving domains at $t=100$ (a), 1000 (b), and 5000 (c) for $\tau=1.7$, $\gamma_1=0.4$, and $\gamma_2=0.2$. The arrow in (b) and (c) indicate the propagating direction.

$=0.4$, $\gamma_2=0.2$, $\gamma_3=0.01$, and $D=1.0$. Note that the growth of long wavelength fluctuations is suppressed, since Re $\lambda(0)$ is always negative.

We now numerically solve Eqs. (3) and (4) in two dimensions for several sets of parameters τ, γ_1, and γ_2, and the other parameters are fixed at $D=1$ and $\gamma_3=0.01$. The computation has been carried out on a 128×128 square lattice with the mesh size $\Delta x=0.5$ using the finite difference Euler scheme with a fixed time step $\Delta t=10^{-3}$ (we have also done the simulation with $\Delta t=10^{-4}$ and observed no qualitative difference in the results). We have used periodic boundary conditions and chosen as initial conditions the homogeneous states with small random perturbations that satisfy $\langle\psi\rangle=\psi_0$ and $\langle\phi\rangle=\phi_0$.

For the parameters below the solid or dashed lines in Fig. 1, no pattern appears asymptotically. Above the dashed line, we have observed stationary patterns due to the Turing instability. The pattern obtained for $\tau=1.4$, $\gamma_1=0.2$, and $\gamma_2=0.2$ ($\psi_0=0.0, \phi_0=0.091$) has a lamellar structure and that for $\tau=0.6$, $\gamma_1=0.04$, and $\gamma_2=0.02$ ($\psi_0=-0.14, \phi_0=0.43$) has a hexagonal structure.

On the other hand, above the solid line, we have observed traveling lamellar and hexagonal patterns. Figure 3 shows three snapshots of the system at $t=100$ (a), 1000 (b), and 5000 (c) for $\tau=1.7$, $\gamma_1=0.4$, and $\gamma_2=0.2$ ($\psi_0=-0.023, \phi_0=0.070$). In Fig. 3 as well as in Fig. 4 below, the value of ψ is shown in gray scale, increasing from black to white. At the early stage irregular patterns with motions of distorted standing waves are formed [Fig. 3(a)]. After that, partially coherent lamellar structures that are traveling emerge [Fig. 3(b)]. The system eventually reaches the state in which the lamellar structure extended to the whole system is traveling at a constant speed [Fig. 3(c)]. These behaviors

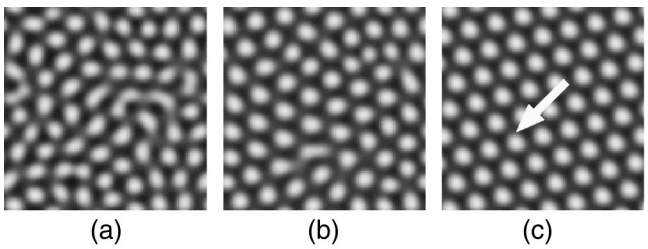

FIG. 4. Snapshots of the moving domains at $t=100$ (a), 1000 (b), and 5000 (c) for $\tau=1.8$, $\gamma_1=0.4$, and $\gamma_2=0.02$. The arrow in (c) indicates the propagating direction.

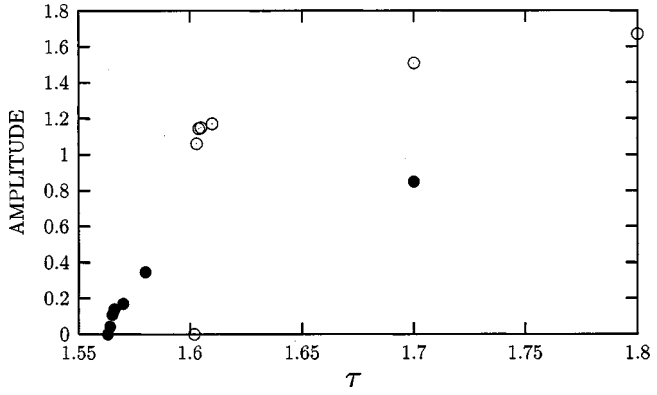

FIG. 5. Amplitudes of ψ defined by the difference of maximum and minimum ψ in the traveling state for the lamellar (closed circles) and hexagonal (open circles) patterns as functions of the control parameter τ.

are similar to those reported by Hildebrand and co-workers [10] in the surface chemical reaction systems. The speed of the traveling structure in Fig. 3(c) is about 0.15, which is close to the phase velocity 0.16 determined by the linear analysis.

Next we show the result for $\tau=1.8$, $\gamma_1=0.4$, and $\gamma_2=0.02$ ($\psi_0=-0.31, \phi_0=0.34$) in Fig. 4. At the early stage, dropletlike domains irregularly move accompanied with breakups and coalescence of domains [Fig. 4(a) and 4(b)] and finally form a regular hexagonal pattern traveling in one direction at a constant speed (about 0.096) [Fig. 4(c)].

In Fig. 5 we plot the amplitudes of ψ defined by the difference of maximum and minimum ψ for the lamellar (closed circles) and hexagonal (open circles) patterns as functions of the control parameter τ. This result indicates that, within the numerical accuracy, the bifurcation to the traveling lamellar pattern is supercritical, whereas formation of traveling hexagons is subcritical.

Now we briefly discuss the formation of traveling hexagons. From the above result we expect that Eqs. (3) and (4) (with $D_\psi=0$) have a solution in the form $\psi(\mathbf{r},t)=\hat{\psi}(\mathbf{r}-\mathbf{V}t)$, $\phi(\mathbf{r},t)=\hat{\phi}(\mathbf{r}-\mathbf{V}t)$, with a traveling velocity $\mathbf{V}$. Here we make the approximation that the functions $\hat{\psi}(\mathbf{r})$ and $\hat{\phi}(\mathbf{r})$ are represented in terms of the lowest Fourier modes as

$$\hat{\psi}(\mathbf{r})=\sum_{k=-3}^{3}\hat{\psi}_{\mathbf{q}_k}e^{i\mathbf{q}_k\cdot\mathbf{r}},\qquad \hat{\phi}(\mathbf{r})=\sum_{k=-3}^{3}\hat{\phi}_{\mathbf{q}_k}e^{i\mathbf{q}_k\cdot\mathbf{r}},\quad (12)$$

where $\mathbf{q}_k\equiv(q_c\cos(2\pi/3)k, q_c\sin(2\pi/3)k)$ $(k=\pm1,\pm2,\pm3)$ and $\mathbf{q}_0\equiv\mathbf{0}$. Note that $\hat{\psi}_{\mathbf{q}_0}=\psi_0$, and $\hat{\phi}_{\mathbf{q}_0}=\phi_0$. From Eqs. (3), (4) and (12), we obtain a set of equation for $\hat{\psi}_{\mathbf{q}_k}$, $\hat{\phi}_{\mathbf{q}_k}$, and $\mathbf{V}$. Eliminating $\hat{\phi}_{\mathbf{q}_k}$ and introducing a real amplitude A_k and a phase θ_k as $\hat{\psi}_{\mathbf{q}_k}=A_k\exp(i\theta_k)$, we finally obtain

$$\Omega(\omega_k)A_k=\mu A_k-3q_c^2[2\psi_0A_lA_me^{-i\varphi}+A_k^3+2(A_l^2+A_m^2)A_k] \quad (13)$$

for $k=1,2,3$ $[l,m=k+1,k+2 \pmod 3]$ with

$$\Omega(\omega) \equiv \frac{\omega^2 - \omega_c^2}{\omega^2 + a^2}(a - i\omega), \tag{14}$$

where $\varphi \equiv \theta_1 + \theta_2 + \theta_3$, $\mu \equiv -q_c^2(Dq_c^2 - \tilde{\tau}) - (\gamma_1 + \gamma_2 + \gamma_3)$, $\omega_k \equiv \mathbf{q}_k \cdot \mathbf{V}$, $a \equiv -(\gamma_2/2) - \gamma_3$, and $\omega_c \equiv \mathrm{Im}\,\lambda(q_c)$ is the critical frequency at the Hopf bifurcation point. Note that two of the three phase variables θ_k are arbitrary and only the sum φ is determined by the above equations. Therefore, Eqs. (13) and (14) under the condition $\omega_1 + \omega_2 + \omega_3 = 0$ determine A_k, φ, and $\mathbf{V}$. If we assume that the solution $\hat{\psi}(\mathbf{r} - \mathbf{V}t)$ has the mirror symmetry with respect to the direction of $\mathbf{V}$, we may have two types of solutions: (I) When $\mathbf{V}$ is perpendicular to $\mathbf{q}_1$, $\omega_1 = 0$ and $\omega_2 = -\omega_3$; (II) When $\mathbf{V}$ is parallel to $\mathbf{q}_1$, $\omega_1 = -2\omega_2$ and $\omega_2 = \omega_3$. The above two cases of type I and II have been observed in Refs. [13] and [14], respectively. Our numerical result shown in Fig. 4(c) corresponds to type II.

In the type-II case, we may set $A_2 = A_3$ by symmetry. Numerically solving Eqs. (13) and (14) under this condition, we obtain A_k, ω_k, and φ as functions of μ. In Fig. 6 we plot A_1, A_2 for $\gamma_1 = 0.4$, $\gamma_2 = 0.02$, $\gamma_3 = 0.01$, and $D = 1$. There are two branches of the solution, the upper two lines and the lower two lines in Fig. 6. Since our simulation shows a subcritical bifurcation, the solution on the upper branch can be regarded as that for the stable traveling hexagons. In fact, this solution gives the traveling speed 0.099, which is close to the observed value 0.096 in the simulation.

In conclusion, we have proposed a different model of phase-separating reactive mixtures, which leads to emergence of self-propulsion of domains. Our numerical simulations in two dimensions have shown that the lamellar and hexagonal structures can propagate coherently above Hopf bifurcation points at finite wave numbers. We have also analyzed the equations of the amplitudes of the lowest Fourier modes for the traveling hexagons and obtained the results consistent with our simulation. However, to complete our analysis, we need further discussion about the stabilities of the solutions. Details including the theory for oscillating lamellar structures will be published elsewhere [17].

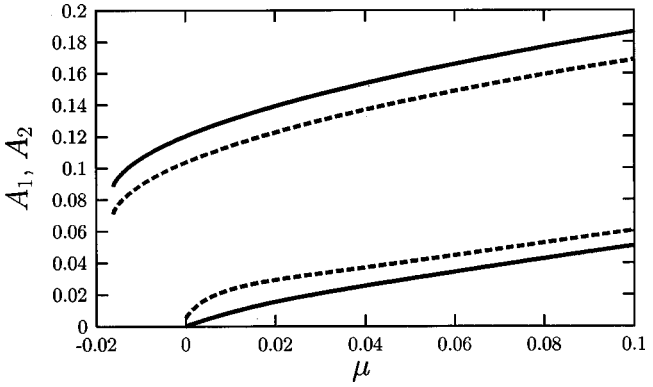

FIG. 6. Numerical solution of Eqs. (13) and (14) in the type-II case. Two branches of the solution for A_1 (solid lines) and A_2 (dashed lines) are plotted as functions of μ.

The authors are grateful to A. Mikhailov for his valuable discussion. This work was supported by the Grant-in-Aid of Ministry of Education, Science and Culture of Japan, the Special Contraction Fund for Promoting Science and Technology from the Agency of Science and Technology of Japan, and partially by a grant from the JSPS Research for the Future Program, Computational Science and Engineering.

[1] M.C. Cross and P.C. Hohenberg, Rev. Mod. Phys. **65**, 851 (1993).
[2] D. Walgraef, *Spatio-Temporal Pattern Formation* (Springer, New York, 1997).
[3] J.E. Pearson, Science **261**, 189 (1993).
[4] K.J. Lee, W.D. McCormick, J.E. Pearson, and H.L. Swinney, Nature (London) **369**, 215 (1994).
[5] J. D. Gunton, M. San Miguel, and P. S. Sahni, in *Phase Transitions and Critical Phenomena*, edited by C. Domb and J. L. Lebowitz (Academic Press, New York, 1983), Vol. 8.
[6] S.C. Glotzer, E.A. Di Marzio, and M. Muthukmar, Phys. Rev. Lett. **74**, 2034 (1995).
[7] J. Verdasca, P. Borckmans, and G. Dewel, Phys. Rev. E **52**, R4616 (1995).
[8] M. Motoyama and T. Ohta, J. Phys. Soc. Jpn. **66**, 2715 (1997).
[9] Q. Tran-Cong and A. Harada, Phys. Rev. Lett. **76**, 1162 (1996).
[10] M. Hildebrand, A.S. Mikhailov, and G. Ertl, Phys. Rev. Lett. **81**, 2602 (1998).
[11] A. S. Mikhailov, M. Hildebrand, and G. Ertl, in *Coherent Structures in Classical Systems*, edited by M. Rubi *et al.* (Springer, New York, 2001) and references cited therein.
[12] Y. Tabe and H. Yokoyama, Langmuir **11**, 4609 (1995).
[13] I. Daumont, K. Kassner, C. Misbah, and A. Valance, Phys. Rev. E **55**, 6902 (1997).
[14] C.B. Price, Phys. Rev. E **55**, 6698 (1997).
[15] M. Bahiana and Y. Oono, Phys. Rev. A **41**, 6763 (1990).
[16] T. Ohta and K. Kawasaki, Macromolecules **19**, 2621 (1986).
[17] T. Okuzono and T. Ohta (unpublished).